Effects of Cold Soaked Fuel Frost on Lift Degradation during Simulated Take-off

Pekka Koivisto

Effects of Cold Soaked Fuel Frost on Lift
Degradation during Simulated Take-off

Pekka Koivisto

Aalto University Department of Applied Mechanics

FOREWORD

This research report is focused on the characteristics of Cold Soaked Fuel Frost, which is an important subject in aviation safety. It forms part of the third year studies in the Icewing project initiated by the Finnish Transport Safety Agency, Trafi.

The research was performed by the team of Arteform Oy, headed by MSc Juha Kivekäs.

Helsinki, September 15th 2015

Erkki Soinne

Chief Adviser, Aeronautics

Finnish Transport Safety Agency, Trafi

Index

ABSTRACT

ABSTRACT

Effects of Cold Soaked Fuel Frost on wing section lift degradation were studied in Aalto University Low Speed Wind Tunnel during winter period 2013-14. Cold Soaked Fuel Frost (CSFF) is a frost created only on the wing fuel tank area during an airliner turnaround time due to the fuel that is considerably colder than the surrounding air. The wind tunnel model used in the study was a three element two dimensional rotating wing section with a chord of 0.65 m. The wind tunnel test section is 2 m x 2 m. The tests conducted consisted of take-off simulations with an approximately linear acceleration up to the speed of 60 m/s (120 kt) followed by a rotation to an predetermined angle of attack for an additional 30 s. The frost on the fuel tank area was real frost not a simulated equivalent sand paper roughness as used in all previous published studies. Several different frost thicknesses ranging from k = 0.07 mm (k/c = 0.01 %) to k = 0.65 mm (k/c = 0.1 %) were generated for the tests. A time dependency of the frost effects due to frost sublimation and melting in air stream was detected which showed the transiency of the lift degradation. This transiency varied strongly with the ambient air temperature. The air temperatures (OAT) varied from -5.5°C to + 11 °C. To compare the real frost test results with a simulated frost there was one test conducted with a fixed sand paper roughness of k = 0.082 mm.

Nomenclature

AAT	Aerodynamic Acceptance Test
c	Wing chord
C_L	Lift coefficient
CSFF	Cold Soaked Fuel Frost, frost on wing surfaces at wing fuel tank area generated by cold fuel
k	Frost thickness
L	Lift force, force perpendicular to the airflow
OAT	Outside air temperature
PEP	Performance Engineer's Program
q	Dynamic pressure
RH	Relative Humidity
S	Wing reference area
x/c	Chordwise relative coordinate, leading edge x/c=0, trailing edge = 1
V_1	Decision speed
V_{1sg}	1 g stalling speed
V_R	Rotation speed
V_2	Take-off safety speed
α	Angle of attack
α_i	Electronically indicated angle of attack
α_m	Visually measured angle of attack

1 Introduction

There is a clear difference between the operative regulations of US and Europe considering the frost related wing contamination restrictions on take-off. The US regulation (14 CFR 121.629(b)) is undisputed on deposits of frost whereas the European regulation (EU-OPS 1.345 (b)) allows a contamination, provided it does not have any adverse effect on the aircraft aerodynamic performance or controllability. The regulatory differences are described in more detail in Chapter 6.1. This window of opportunity of non-US regulations – especially European and Canadian regulations - has been utilized by Boeing. The Boeing 737 NG model is authorized for limited Cold Soaked Fuel Frost on wing upper surface at take-off as defined in the AFM (Aircraft Flight Manual)[1].

There is a lot of published studies of contamination effects on wing aerodynamics. Part of these studies is addressing the problem of frost[2,3]. Generally however these studies concentrate on situations where the wing upper side is covered with an artificial roughness (sand paper or other) along the whole chord. Most of the studies on frost effects consider the so called Hoar (radiation) Frost utilizing plastic or other artificial grain simulation of the real frost texture. To address rigorously the effects of CSFF the aerodynamic deterioration of a wing should be studied with a real Cold Soaked Fuel Frost located on the applicable area of wing upper surface. It is obvious that Boeing has conducted specific wind tunnel tests to comply with regulations in 737 NG CSFF approval[1] however all the related data is classified and thus does not exist for the general research community. The present study is the first public one on CSFF where the frost examined is actual cold soaked frost.

The present study is based on wind tunnel tests at Aalto University Low Speed Wind Tunnel carried out during January 27th - April 4th 2014 utilizing a rotational 3 element 2 dimensional wing section model. The wing section geometry has been chosen to represent a modern airline wing section.

It is reasonable to compare the aerodynamic degradation caused by CSFF with the corresponding degradation caused by anti/de-icing fluids as these two are the alternatives in real life: either depart with CSFF or de-ice/anti-ice the wing before the departure. As the so called Aerodynamic Acceptance Test (AAT) forms the reference for analyzing the aerodynamic effects of the de/anti-icing fluids the present study applies the methodology adopted in wind tunnel tests performed to compose the SAE AS 5900[4]. This means simulated take-off runs in a wind tunnel with accelerating airspeeds up to a typical airliner rotation speed, and then rotating the wing model to an angle of attack representing a lift coefficient typical in an One Engine Out situation at the speed of V_2. The aerodynamic degradation is determined by measuring forces acting on the wing model throughout the wind tunnel run.

2 Objectives

The objectives of the present study were to evaluate the effects of CSFF on lift degrada-tion of an airliner during a simulated take-off. The parameters varied in the tests were the initial mean thickness of the frost layer and the Outside Air Temperature (OAT) which is the wind tunnel air temperature in this case. As there is no temperature control in Aalto University Low Speed Wind Tunnel the prevailing Outside Air Temperature had to be accepted as a daily changing "fixed" parameter.

As this study is not intended to be an exhaustive description of CSFF effects on an air-liner lift degradation during take-off, one important objective is to motivate further studies related on the subject.

3 Test Arrangements

3.1   Wind Tunnel

Aalto University Low Speed Wind Tunnel is a closed circuit wind tunnel with an octagonal test section with dimensions of 2 m x 2 m and a test section length of 4 m. The flow uniformity in the test section is < 0.14 %, and turbulence level <0.1 % of the mean wind tunnel speed.
The massive concrete structures of the wind tunnel ducts are outside the facility building. This makes the tunnel structure during winter time an efficient heat sink and the fan power dissipated during short period take-off run simulation does not increase the test section temperature significantly (< 2 º C). Temperatures in the test section follow roughly the daily outside air temperature (OAT). During the tests of this study the wind tunnel air temperature varied between − 5.5˚C and + 11˚C.

3.2   Wing Section Model

All tests of the present study were conducted with a two dimensional 3 element rotating model that was mounted to a three component balance to measure the aerodynamic lift, drag and pitching moment. The wing section model has the geometry of a DLR-F15[5] profile and a chord of 0.65 m. The model span was 1.5 m which implies an area of 0.975 m^2 (Fig 1.). The model was equipped with endplates to minimize the three dimensionality of the flow. Two dimensionality and absence of flow separations were confirmed by tufts.

The wing model was equipped with a glycol coolant tank to simulate the effect of cold fuel in a wing tank (Fig 2.) The tank was cooled down initially taking the wing model into a deep freezer before mounting it to the test section. There was two copper tubes with attached cooling foils assembled inside the tank with passages on both end plates to enable further cooling of the tank by running liquid nitrogen through the tubes after the model had been mounted to the test section. The coolant tank temperature was monitored via a temperature sensor inside the coolant tank. The surface material on the tank area was painted aluminum whereas the other parts of the wing model consisted of ureol blocks with the same surface paint.

The wing model coolant tank which simulates an airliner fuel tank extends from the relative chord position of x/c = 0.215 to position of x/c = 0.615. The area of the fuel tank is therefore 40% of the reference wing area in the clean configuration.

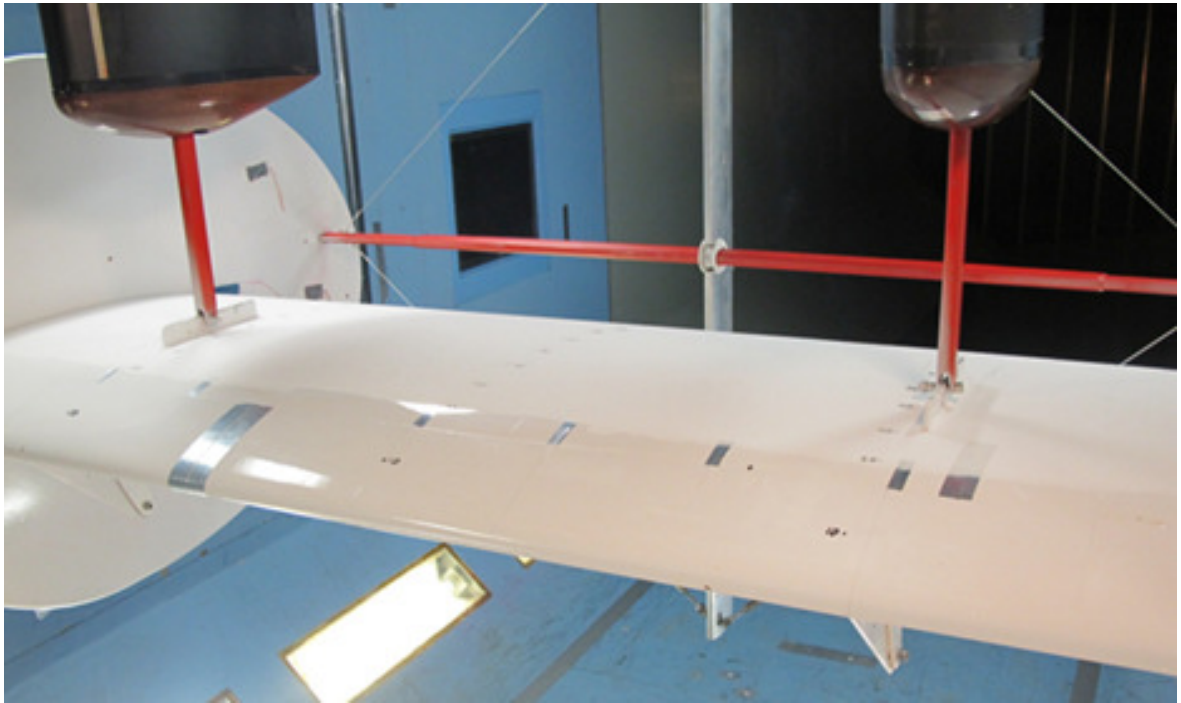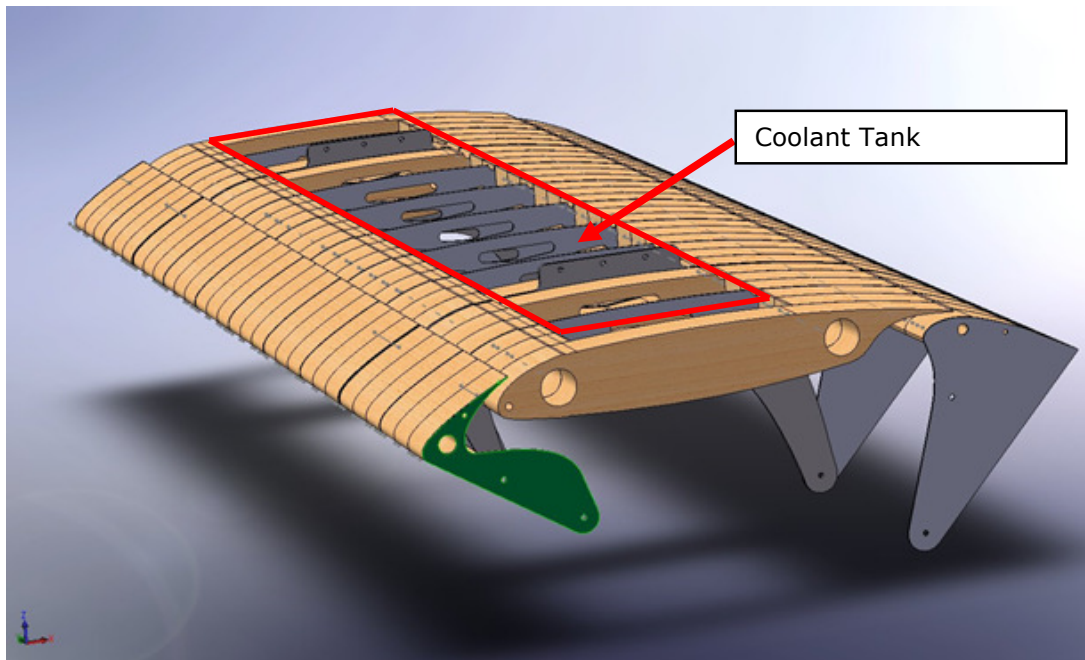**Figure 1.** Rotating wing section model in wind tunnel**.**

Coolant Tank

Figure 2. Structure of wing section model

4 Data Acquisition and Assessment of Measurement Accuracy

There is a standard measuring software in the wind tunnel collecting the wind tunnel temperature, airspeed, dynamic pressure, relative humidity, balance forces and moments (lift, drag and pitching moment in this case) and the wing angle of attack.

The temperature of the coolant tank was measured separately as the intention was to follow the mean temperature during each test and not to coordinate it with the measurement sequence in time.

The effect of frost on the wing tank area on the take-off performance is evaluated by measuring the lift coefficient degradation ΔC_L due to the CSFF contamination. This means sequential C_l - measurements of the clean wing and a contaminated wing. As the result is a difference between the two lift coefficients at the same angle of attack the repeatability of the tests is more relevant than the absolute accuracy of the lift coefficient itself.

The lift coefficient measurements for a clean wing gave well repeatable results at the fixed angle of attack of interest ($8°$). For 20 separate clean wing tests the lift coefficient mean value was 1.281 with standard deviation of 0.0028, which gives a coefficient of variation of 0.219%. In case of cold soaked fuel frost, it was not possible to end up with two similar frost layer to define any repeatability.

5 The Simulation of CSFF

To get the wing model coolant tank area frosted the model was kept overnight in a deep freezer room. During the time the wing model was transported from the freezer and assembled to the wind tunnel test section the coolant tank warmed up inevitably from the initial temperature of -25°C to around -15 °C. As the liquid nitrogen system was not built to be used during the test runs the tank warmed up further some 5 °C during the runs. The tank temperatures on each test are found in Table 2.

During the transport and assembly of the model to the test section there was time for the coolant tank area to get frosted. The "natural" frost layer created on the wing model surface never grew exceeded 0.15 mm. One particular parameter that could not been altered was the wind tunnel air humidity. The Relative Humidity values in the wind tunnel test section varied from 34 % to 86 %. Fig. 3 describes the correlation between the natural frost build up and Relative Humidity.

To grow up the frost mean thickness on the tank area some moisture was generated to the test section using a spray device. This device was utilized in front of the model with simultaneous low wind speeds in the tunnel (5 m/s). By this method a frost thickness up to 0,55mm could be generated. Tests were performed with both natural frost and frost with artificially increased moisture. There is a decomposition of the frost and prevailing conditions in Table 2.

The frost densities or liquid water contents were not measured in this study.

As is seen in Table 2 the tank temperature warms up somewhat during the tests. However, it is well below the freezing point in all tests (-10 °C is the highest tank temperature). The tank temperature differences are not assumed to affect considerably the results of this study.

The first test (T1) on 24.4.2014 failed to give reasonable wind tunnel test results but the frost thickness measurement is valid however.

Table 2. Frost thicknesses generated for the tests. k is the mean frost thickness in mm. SD_k is the standard deviation of k. k/c is the frost thickness as a fraction of wing chord. SD_k/c is the standard deviation of k/c. RH is the Relative Humidity, TT is the coolant tank temperature, OAT is the wind tunnel air temperature. N indicates natural type of frost and AH added humidity type of frost.

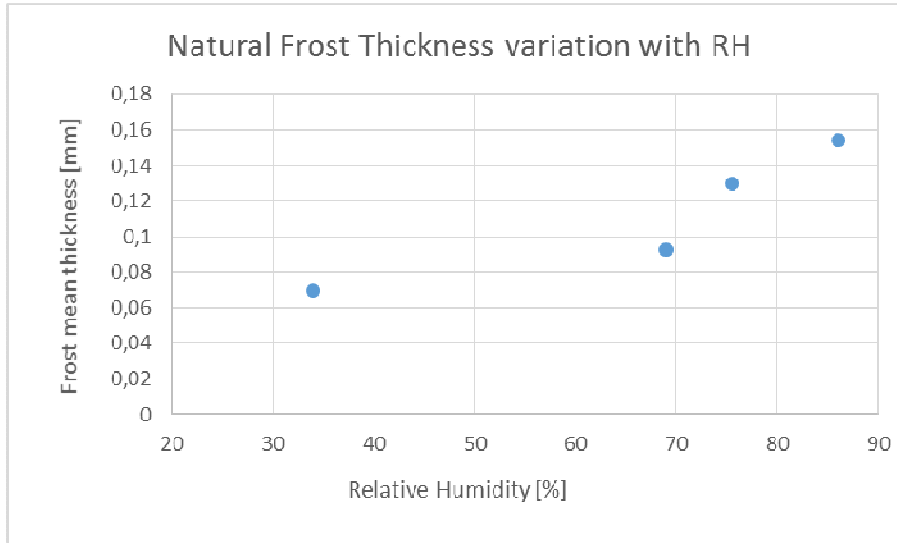| **Day**	Test	k [mm]	SD_k [mm]	1000*k/c	1000*(SD_k/c)	RH [%]	TT [°C]	OAT [°C]	Type
27.1.	T1	0,093	0,022	0,142	0,034	78	-14	-5	N
	T2	0,525	0,375	0,808	0,577		-13	-5	AH
	T3	0,375	0,225	0,57692	0,346		-11	-5	AH
6.2.	T1	0,133	0,093	0,205	0,143	76	-15	-1	N
	T2	0,650	0,187	1,000	0,288		-13	-1	AH
	T3	0,550	0,153	0,846	0,236		-10	-1	AH
13.2.	T1	0,154	0,151	0,237	0,233	86	-15	4	N
	T2	0,475	0,263	0,731	0,405		-13	4	AH
24.4.	T1	0,071	0,026	0,109	0,041	34	-13	11	N
	T2	0,283	0,023	0,436	0,036		-10	11	AH

Figure 3. The natural frost thickness variation with the test section air relative humidity (RH).

Measurement Program

5.1   Lift Degradation as a Take-off Performance Criterion

The objective of a take-off simulation wind tunnel test is to simulate the One Engine Inoperative (OEI) situation where the airliner is flying at the speed of V_2 after lift-off up to the so called "cleaning altitude" at which the flaps and slats are retracted (>400 ft above ground level as per EASA CS 25.121[6] see figure 4).

The effects of frost contamination (EASA and TC Certification Standards) or de/anti-icing fluid application (all Certification Standards including the US FAR 25) to the take-off performance of an airliner have not been addressed. However, a "non-written" policy exists that addresses these contaminants with the requirements considering the inflight icing.

The requirement applied for the frost and de/anti-icing fluid contaminant (common for EASA, TC and FAA) is as follows:
"25.121 (b)(2) Climb one engine inoperative, Take-off; landing gear retracted:
The requirements of subparagraph (b)(1) of this paragraph must be met:
(i) In non-icing conditions; and
(ii) In icing conditions with the "Take-off Ice" accretion defined in Appendix C, if in the configuration of CS 25.121(b) with the "Take-off Ice" accretion:
(A) The stall speed at maximum take-off weight exceeds that in non-icing conditions by more than the greater of 5.6 km/h (3 knots) CAS or 3% of VSR; or
(B) The degradation of the gradient of climb determined in accordance with CS 25.121(b) is greater than one-half of the applicable actual-to-net take-off flight path gradient reduction defined in CS 25.115(b)"

This means that if V_{SR} in the configuration defined by CS 25.121(b) with the "Takeoff Ice" accretion defined in Appendix C to CS-25 exceeds V_{SR} for the same configuration without ice accretion by more than the greater of 3 knots or 3% or the degradation of the

gradient of climb is greater than 0.4 % for 2-engine aircraft, the take-off demonstrations should be repeated to substantiate the speed schedule and distances for take-off in icing conditions. In case of CSFF this requirement is applied as such for frost contamination. In case of de/anti-icing fluids Hill and Zierten[7] evaluated several specific take-off performance criteria following FAR 25 while developing the Aerodynamic Acceptance Test for fluids and ended up to the stall speed part of the above regulation (25.121 (b)(2)(A)).

If frost is considered to remain on the wing considerably above the cleaning altitude (400 ft AGL) it is obvious that there is a possibility that the climb gradient will be more critical than the lift stall speed degradation. However, in a wind tunnel test for a wing model the only relevant restriction to be studied is naturally the stall speed restriction.

The stall speed margin degradation of 3% may be interpreted as a lift coefficient (C_L) degradation of 5.24 % at the selected "lift off" angle of attack. For detailed reasoning of this see Ref 8.

Regarding both de/anti-icing fluid tests and frost tests in wind tunnel the negative temperature gradient during initial climb will not be taken into account. As the standard atmosphere temperature gradient is approximately only 2˚C/1000ft this will not affect considerably the analysis presented here.
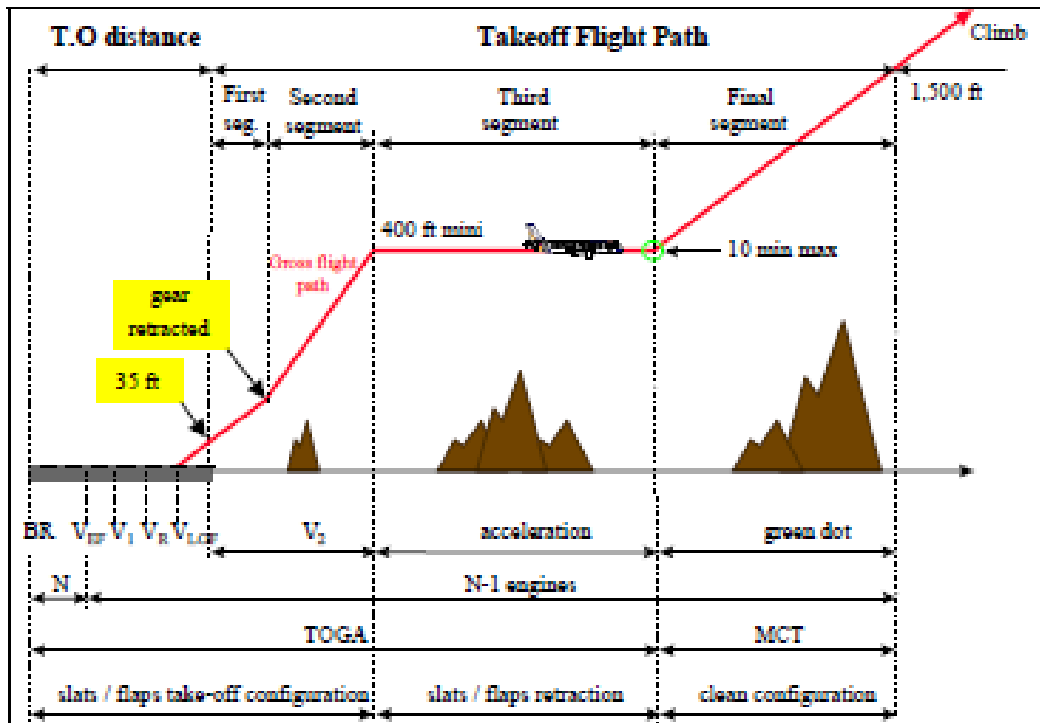
Figure 4. Take-off flight path as per EASA CS 25.12.

5.2   Wing Section Configuration and Take-off Sequence

A take-off sequence (engine failure at speed V_1) of an airliner consists of (see Fig. 4.):

- Acceleration from stand still to the rotation speed (V_R) with a constant pitch attitude during ground roll

- After reaching V_R the pitch attitude is increased to a lift off attitude (normally a predetermined constant value e.g. 15°)

- Once airborne the airspeed is accelerated to V_2 where it remains until reaching the cleaning altitude at which the slats and flaps are retracted

To simulate in a wind tunnel the speed sequence in detail, as given above is too complicated a task. A generally adopted simplification among the AAT –research tests documented[9] is to accelerate the speed from wind tunnel idle speed as linearly as possible to V_2 and then rotate the wing section to a predetermined angle of attack and keep it there for a predetermined time – e.g. 30 s.

The DLR F-15 wing section model was tested with several different slat and flap configurations to find a satisfactory combination of angle of attack and lift coefficient both during ground roll and at speed V_2, which in this case was limited by the maximum wind tunnel speed of 60 m/s (120 kt). After a set of extensive tests, the best configuration appeared to be slats deflected 11°, and flaps 12° which gave the following combinations of angle of attack and lift coefficient (see Ref. 8 for detailed analysis):

- Ground roll (acceleration to 60 m/s) α = 0° and C_L = 0.5

- Speed 60 m/s (V_2) wing section rotated α = 8° and C_L = 1.3

The chosen speed-angle of attack (α) - time sequence was as follows[8] :

- At α = 0 wind tunnel speed is accelerated from idle speed to 60 m/s.
- As soon as the speed has reached 60 m/s it is kept constant and the wing section is rotated at a rate of 3.0°/s to α = 8°
- After α = 8° has been reached the wind tunnel speed is kept at 60 m/s for 40 seconds

Note that in Ref. 8 the angle of attack figures are erroneously 1° and 7.5° which are not consistent with the C_L -α curve shown in Ref 8.

The time used to accelerate the wind tunnel speed to 60 m/s is constant 30 s. A graphical description of the simulated take-off sequence is shown in Fig. 5.
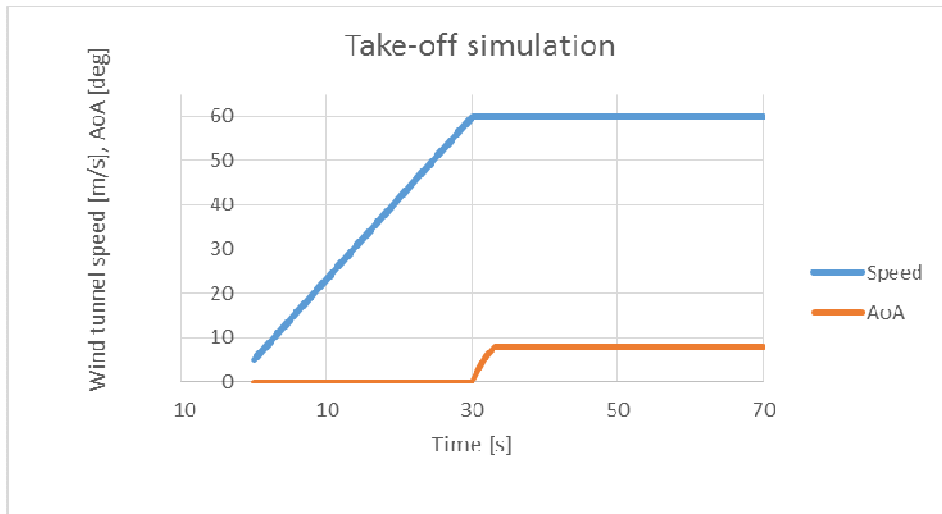

Figure 5. Speed and angle of attack (AoA) sequences.

6 Test Results

6.1   General Qualitative Observations

The progress of frost sublimation and/or melting during the test were tried to be visualized by video, assembled on the roof of the wind tunnel test section. However, the white painting of the model, which originally served the tests with anti-icing fluids, prevented the frost layer changes to be observed.

The changes in the frost layer during the tests were however observed clearly by naked eye through the test section door and were verbally documented. Some photos and video recordings taken at a suitable angle from the wing surface during the tests contributed these observations.

Though the coolant tank situated chord wise between x/c = 0.215 to 0.615 there appeared some very thin frost behind the rearmost line of the coolant tank. This clearly visible frost layer however was mostly thinner than the resolution of the Elcometer thickness gage (=0.025 mm).

According to visual observations the frosted area reduction started mostly from the rear side of the initial frost area. There were two tests done where the frost thickness was measured also after the test. The measurements of the frost thicknesses and the frost area showed that the relative reduction of the frost area after the tests was clearly larger than the reduction of the mean thickness of the frost.

There appeared to be an even thicker frost layer (1-1.5 times) on the lower surface compared to the upper surface of the wing model. However, the effect of this frost was omitted based on Ref. 10.

6.2   Lift Degradation after Rotation

To determine the lift degradation for different parameters the clean wing case was measured after each frost test to eliminate different daily changing factors on the results. In the following the lift degradation variation in time is presented in figures where time point 0 represents the situation where rotation has just ended and angle of attack $\alpha = 8°$ has been reached. Results are presented in per cents (%) of clean wing lift coefficient. As reasoned above in chapter 6.1 an acceptable lift coefficient loss may be considered as 5.24 %.

The results of lift coefficient degradation tests are collected into Figures 6 – 9. The wind tunnel air temperature (OAT) depends on the test day as detailed in Table 2.

Figure 6 shows the test results at the coldest wind tunnel temperature in this study. The decrease of lift degradation during 30 s after rotation is approximately one percentage point and the alteration is almost linear. Note that the relative frost thickness degradation during the tests in cases of k/c = $0.577*10^{-3}$ and $0.808*10^{-3}$ was below 5.0 % whereas the alteration in frost area was about 25-30%. The exact estimation of the frost area was difficult due to the non-uniform edge of the frost area after the test.

Lift degradation at an air temperature of -1°C is shown in Figure 7. As in Figure 6 the lowest frost thickness (Natural frost) produces a lift coefficient degradation of well be-

low the accepted limit of 5.24%. Also the slope of the curve is somewhat steeper than in the thicker frost layer cases (with added humidity).

In Figure 8 the air temperature is +4 $^{\circ}$C. With the highest Relative Humidity value of this study the natural frost built up in this particular case was the thickest (see Fig. 3). The two quite different frost layers created (k/c = $0.237*10^3$ and $0.731*10^3$) led to initial degradations
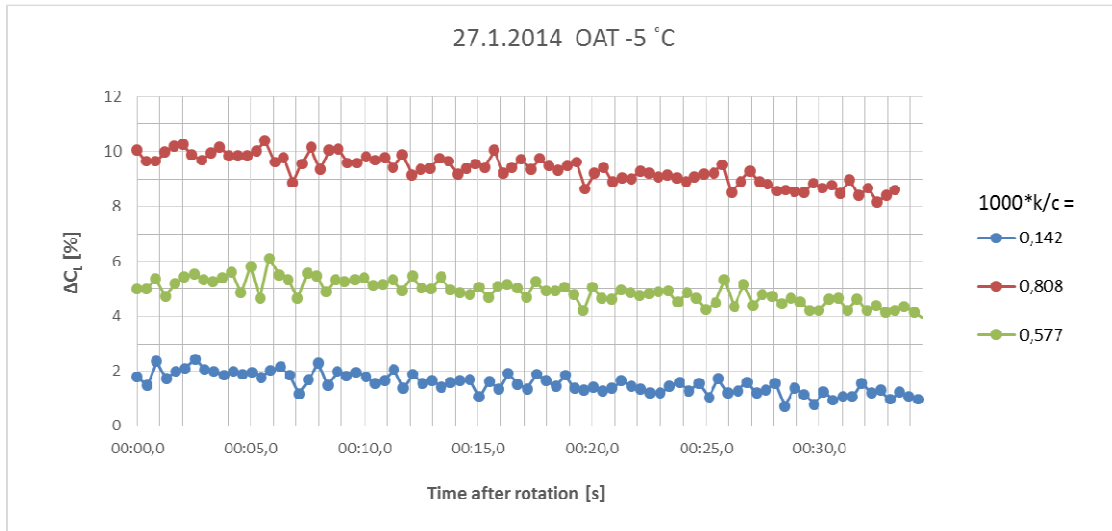

Figure 6. Lift coefficient degradation variation with time after rotation for three different frost thickness at a wind tunnel air temperature of -5°C. For other conditions see Table 2.
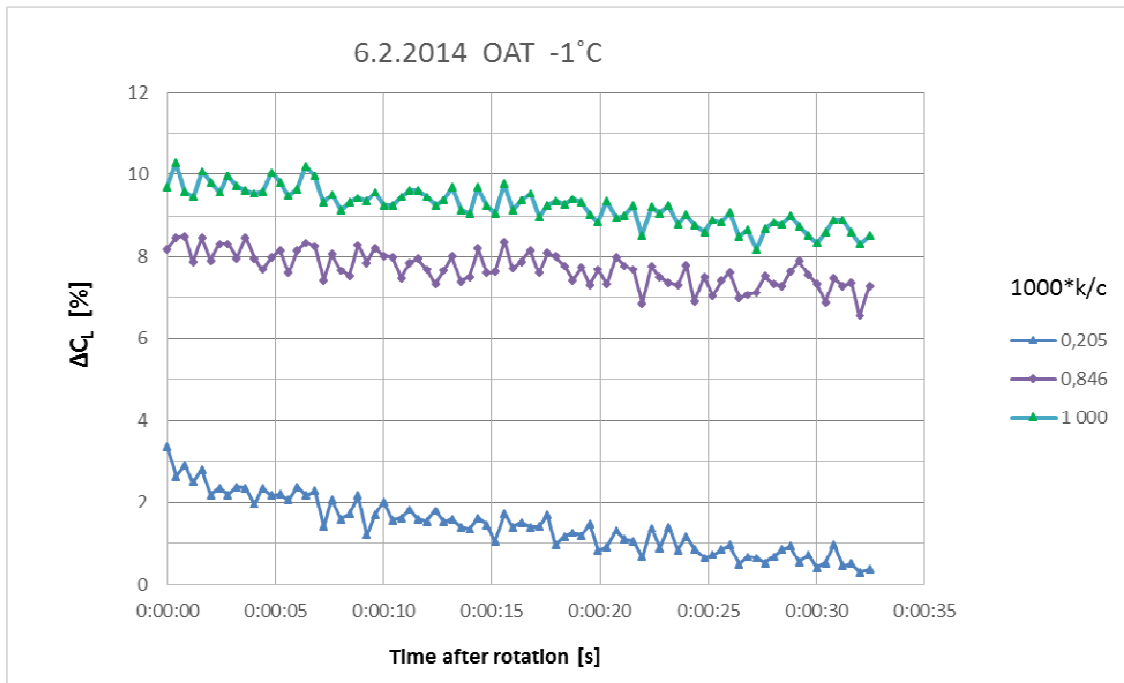

Figure 7. Lift coefficient degradation variation with time after rotation for three different frost thickness at a wind tunnel air temperature of -1°C. For other conditions see Table 2.

of lift coefficient with only 1 percentage point difference. However, in case of the thinner frost (natural frost) the lift degradation decreases clearly more progressively within the first 30 s. Note that the curves have merged at time 35 s.

The highest wind tunnel air temperature in this study was +11 ˚C. Lift degradation at this temperature is shown in Figure 9. Only one frost case was tested at this
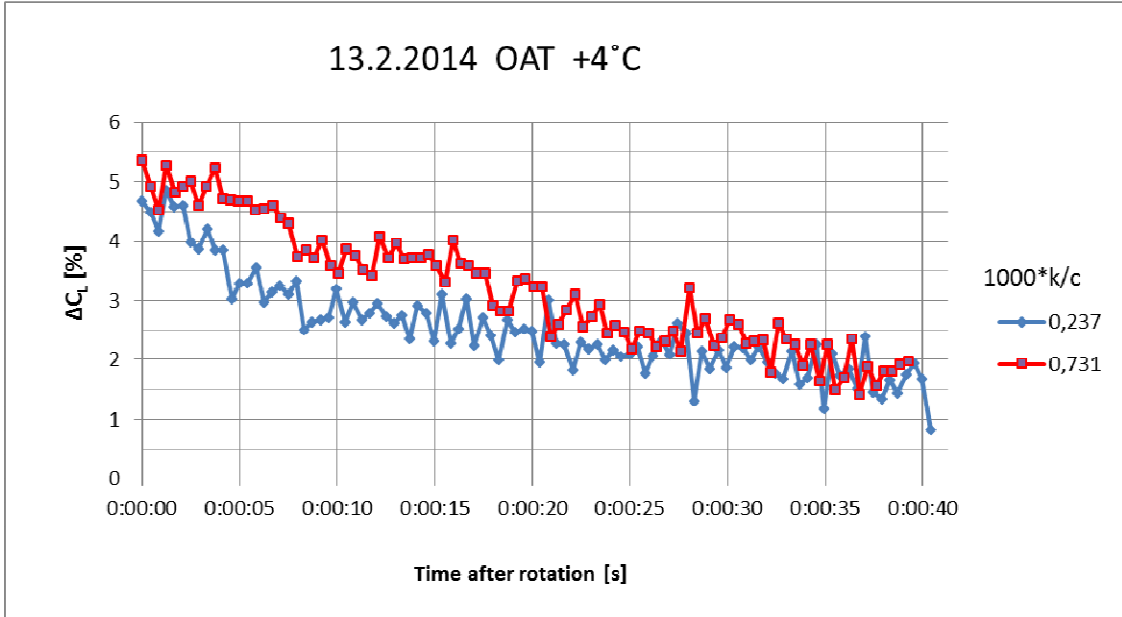

Figure 8. Lift coefficient degradation variation with time after rotation for three different frost thickness at a wind tunnel air temperature of +4˚C. For other conditions see Table 2.
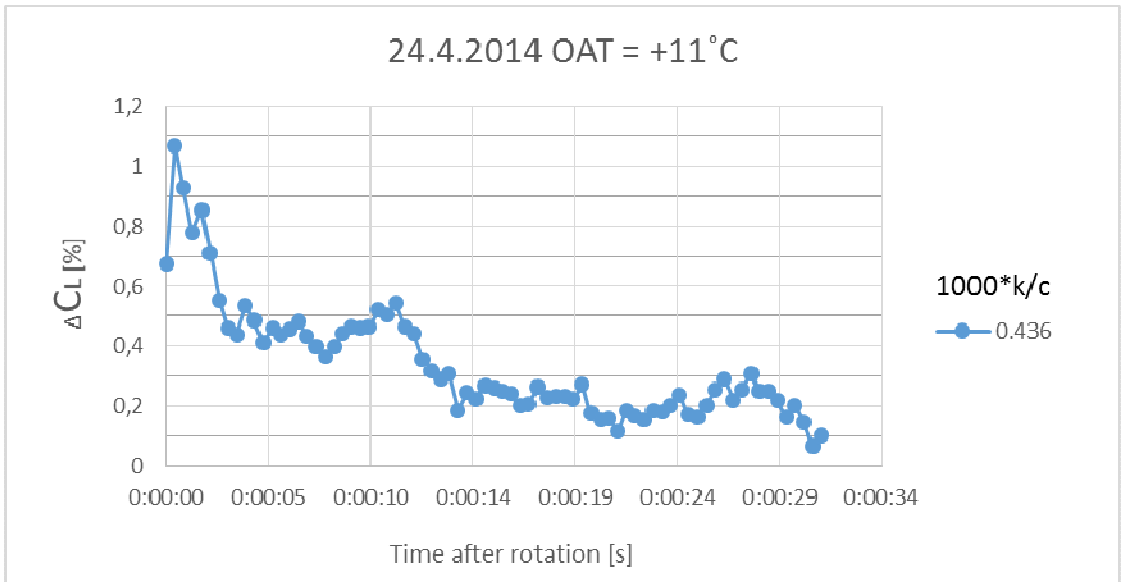

Figure 9. Lift coefficient degradation variation with time after rotation for three different frost thickness at a wind tunnel air temperature of +11˚C. For other conditions see Table 2.

temperature. The lift coefficient degradation just after rotation is much lower than for even thinner frost layers at colder temperatures. The effect of frost is practically vanished after 30 s from the rotation. It is obvious that there has been some decrease of frost layer thickness and area already at the take-off roll before the rotation due to relatively high air temperature. The role of take-off roll phase in the low value of lift degradation at rotation is analyzed in the next chapter.

6.3   Lift Degradation during Take-off Roll

The lift coefficient degradation at and after the lift off correlates fairly well with the initial frost roughness in results of Figures 6 to 8. However, the case where OAT is +11°C seems to deviate from this correlation. To determine the possible contribution of take-off roll phase to the apparently low value of lift coefficient degradation at and after rotation all the take-off roll phase (accelerating airspeed with constant pitch angle) lift coefficients were analyzed.

There is a typical lift coefficient degradation with time during take-off roll as shown in Figure 10. During the first 10-15 seconds the lift coefficient data is considerably noisy and the fluctuation levels from the mean value are so high that the first three seconds are left out of the figure to get the scale reasonable for the last 15 seconds. This may be due to low Reynolds number related phenomena such as laminar separation and boundary layer transition movement. However, after the first 15 seconds, though not steady, the measured lift coefficients are less deviating. Excluding the case (day 24.4.2014) where the air temperature was +11°C all measurements gave a result resembling Figure 10. The lift degradation during the take-off roll does not have a particular trend but the mean value remains constant though the fluctuation is considerably high.

In contrast to all the other measured lift coefficient degradations the case of day 24.4.2014 gave a curve shown in Figure 11. The measured lift coefficients are just as fluctuating as in the case of Figure 10 however a clear trend may be recognized. Taking time averaged lift degradation values from time intervals 15-17 seconds and 28 - 30 seconds after starting the take-off one gets a decrease in lift degradation of 2.55 percentage points. This is naturally not transferable directly to the initial lift degradation after rotation but implicates however that the frost effect alters the lift coefficient considerably already during the take-off run which explains the anomaly of lift degradation after rotation on 24.4.2014 (OAT=+11°C) compared to all the other days.
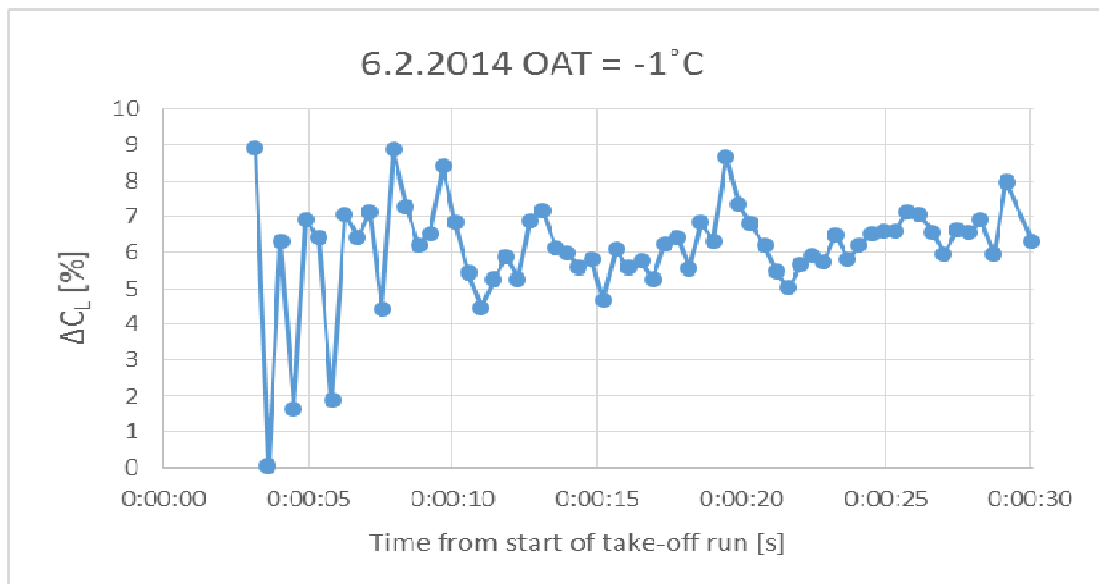
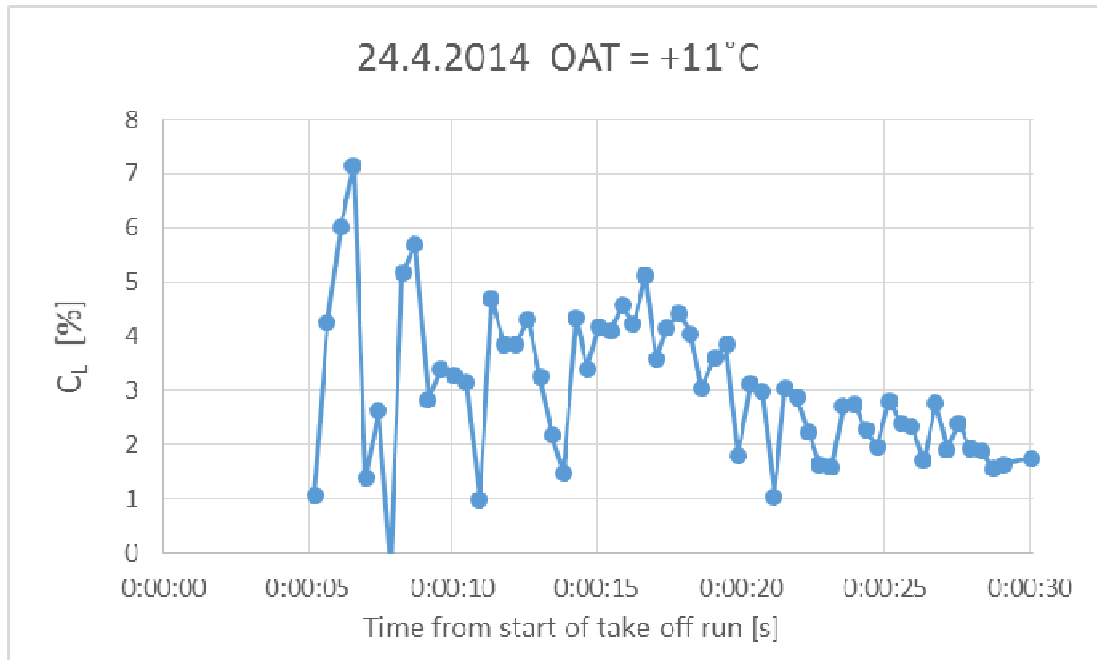**Figure 10.** Lift coefficient degradation during take-off run. k/c = 1.0*10^3.

Figure 11. Lift coefficient degradation during take-off run. k/c = 0,436*10^3.

6.4   Real Frost compared to Sandpaper Roughness

To evaluate the frost induced effect on lift degradation one test was done with a fixed known sandpaper roughness. In this test a P180 sandpaper was assembled on the wing tank area. It was assumed that equivalent roughness was the specified roughness value of the sandpaper P180 i.e. k=0.082mm which is equivalent to k/c=0.126*10^3.

The sand paper P180 roughness on wing tank area gave a lift coefficient degradation time average within 30 s after take-off of 0.854% with a standard deviation of 0.244%. The take-off roll phase gave a very fluctuating result – the time average from 10 s after start of take-off roll to rotation (30 s) was 0.9% with a standard deviation of 0.95%.

There is a summary of lift coefficient degradations with different frost thicknesses of the present study in Figure 12. The sandpaper roughness of this study is included. There are also two results from Ref. 11 included in Fig. 12. In Ref 11 the lift degradation of a NACA63$_2$-015 wing section was measured when the wing upper side was applied with a roughness extending from x/c = 0.2 to the trailing edge. When comparing the rough-ness induced lift degradation between different wing sections it is essential that the chord wise distributed roughness has equal starting point. The lift degradation tests in Ref. 11 were done at an angle of attack of 8.5°.

In the "Modified Value" point in Figure 12 the ΔC_L – value is a sum of lift coefficient val-ue change during take-off roll and the initial lift degradation just after rotation. It is not strictly comparable with the other data points but however straightens up the otherwise anomalous result of Figure 9 where obviously part of the frost has disappeared during the take-off roll.
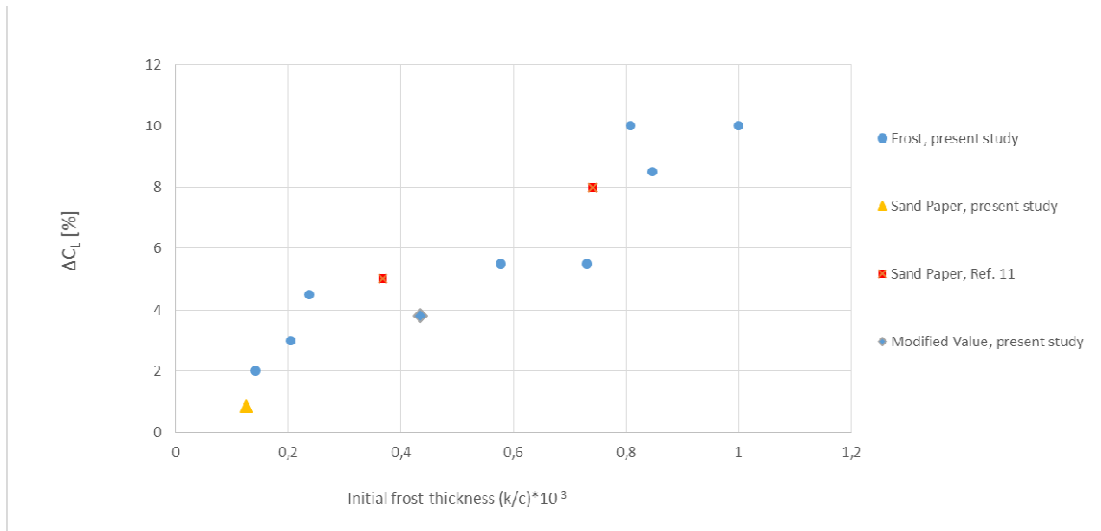
Figure 12. Lift coefficient degradation [%] variation with initial frost thickness or sand paper roughness in $(k/c)*10^3$. The blue round marks represent results from present study, yellow triangle the sandpaper result of present study, red squares the results of Ref. 11 and the green diamond is a modified value of test result from day 24.4.2014 ($+11^\circ$C). See text for details.

6.5   The effect of Temperature on Lift Recovery

One of the objectives of this study was to show that there is a temperature dependent transiency present in the lift degradation effect of frost. This transiency follows from sublimation and/or melting of the frost during take-off. The test results shown in Figures 6 to 9 clearly show that after rotation the lift coefficient is partly recovered i.e. the lift coefficient degradation decreases with time. This decrease is clearly dependent on the prevailing air temperature (OAT) Which is shown in Fig. 12. In Fig 12. the blue circles represent the results of Figures 6 to 9. The amber square is a modified value where the total recovery of lift coefficient is a sum of the recovery during take-off roll and 30 s after rotation. The relationship between lift recovery and temperature is obvious even without the speculative modified result of day 24.4.2014 with OAT of +11 $^\circ$C (Fig. 13).
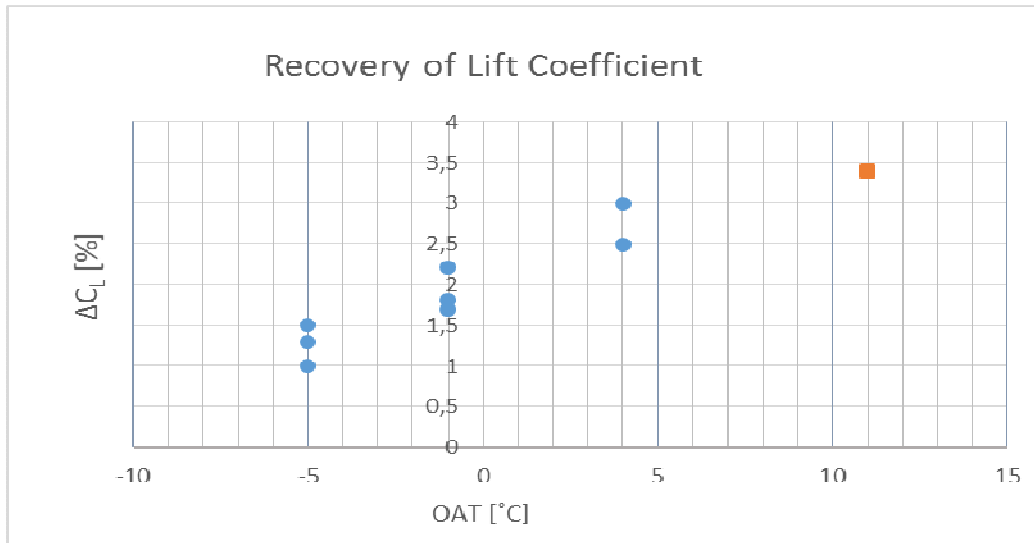
Figure 13. The variation of the recovery of the lift coefficient during first 30 s after rotation with air temperature. Note: the red square represents a data point where lift coefficient recovery is a sum of recovery during take-off roll and recovery 30 s after rotation.

7 Conclusions

Wind tunnel experiments for a DLR-F15 three element wing section model were conducted at Aalto University Low Speed Wind Tunnel facility during the winter period 2013-2014. Objectives were to study the lift degradation and its alteration on a wing section during take-off caused by Cold Soaked Fuel Frost. The frost effect transiency after rotation (take-off) were demonstrated in tests with air temperatures varying from -5˚C to +11 ˚C. The effect of frost reduced with time and temperature after rotation. At air temperature of +11 ˚C part of the frost effect vanished already during take-off roll and almost all the rest of the frost after the rotation.

The recovery from frost induced lift degradation after the rotation is probably caused by frost sublimation and melting. The lift degradation was shown to vary clearly with the air temperature.

This study may be considered as a motivation for further research on this topic and the following issues should be addressed in future:

- frost density or liquid content effect on lift degradation – in this study only the frost layer thickness was determined
- The fuel tank temperature effect on lift degradation. In this study only temperatures between -10 ˚C to -15 ˚C were considered
- theoretical background for frost sublimation and melting on a wing

When comparing the lift degradation due to frost and anti-icing fluids[8] it is obvious that there are occasions in normal airliner winter operations where a strict "clean wing concept" does not enhance safety but however load the environment and economics of flights.

References

1. Adrian, P., Brightwell J.: Operating Boeing 737-NG with Cold – Soaked Fuel Frost", Presentation given at EASA Annual Safety Conference at Cologne, Germany, 15-16th October 2013.
2. Ljungström, B.L.G.: "Windtunnel investigation of simulated hoar frost on a two-dimensional wing section with and without high lift devices." Report FFA-AU-902, April 1972
3. Kind, R.J., Lawrysyn, M.A.: "Performance Degradation due to Hoar Frost on Lifting Surfaces." Canadian Aeronautics and Space Journal, Vol 38, No. 2, June 1992.
4. "Standard Test Method for Aerodynamic Acceptance of SAE AMS 1424 and SAE AMS 1428 Aircraft Deicing/ Anti-icing Fluids", AS5900 Rev.B , SAE International, 26 July 2007.
5. Wild, J.: "Experimental investigation of Mach- and Reynolds-number dependencies of the stall behavior of 2-element and 3- element high-lift wing sections", AIAA 2012-0108, 50th AIAA Aerospace Sciences Meeting including the New Horizons Forum and Aerospace Exposition 09 - 12 January 2012, Nashville, Tennessee
6. Certification Specifications and Acceptable Means of Compliance for Large Aeroplanes, CS-25 Amendment 13, 10 June 2013, Annex to ED Decision 2013/010/R, Amendment
7. Hill, E.G., and Zierten, T.A., "Aerodynamic Effects of Aircraft Ground Deicing /Anti - Icing Fluids," Journal of Aircraft, V o l. 3 0, N o. 1 , Jan. -Feb., 1993
8. Koivisto, P. "Effects of Anti-icing Treatment on Lift Degradation during Simulated Take-off" Trafi Publications 25/2013.
9. Broeren, A., Riley, J: "Review of the Aerodynamic Acceptance Test and Application to Anti-icing Fluids Testing in the NRC Propulsion and Icing Wind Tunnel" NASA TM 2012-216014, Aug. 2012.
10. Bragg, M.B. et al: "Effect of Underwing Frost on a Transport Aircraft Airfoil at Flight Reynolds Number.", Journal of Aircraft, Vol 31, No. 6, Nov.-Dec., 1994.
11. Oolbekkink, B., Volkers, D.F.: "Aerodynamic Effects of Distributed Roughness on a NACA 63_2-015 Airfoil.", AIAA-91-0443, 29th Aerospace Sciences Meeting, Jan 7.-10., 1991, Reno, Nevada.